Investigation of writing error in staggered heated-dot magnetic recording systems

W. Tipcharoen, C. Warisarn, D. Tongsomporn, D. Karns, and P. Kovintavewat

Citation: AIP Advances **7**, 056511 (2017); doi: 10.1063/1.4977762
View online: http://dx.doi.org/10.1063/1.4977762
View Table of Contents: http://aip.scitation.org/toc/adv/7/5
Published by the American Institute of Physics

Investigation of writing error in staggered heated-dot magnetic recording systems

W. Tipcharoen,[1] C. Warisarn,[1] D. Tongsomporn,[2] D. Karns,[3] and P. Kovintavewat[4]
[1]*College of Advanced Manufacturing Innovation, KMITL, Bangkok 10520, Thailand*
[2]*Seagate Technology (Thailand), Teparuk, Mueang, Samutprakarn 10270 Thailand*
[3]*Seagate Technology US NRM Facility, Bloomington, Minnesota 55435, USA*
[4]*Data Storage Technology Research Center, NPRU, Nakhon, Pathom 73000, Thailand*

(Presented 1 November 2016; received 23 September 2016; accepted 25 November 2016; published online 28 February 2017)

To achieve an ultra-high storage capacity, heated-dot magnetic recording (HDMR) has been proposed, which heats a bit-patterned medium before recording data. Generally, an error during the HDMR writing process comes from several sources; however, we only investigate the effects of staggered island arrangement, island size fluctuation caused by imperfect fabrication, and main pole position fluctuation. Simulation results demonstrate that a writing error can be minimized by using a staggered array (hexagonal lattice) instead of a square array. Under the effect of main pole position fluctuation, the writing error is higher than the system without main pole position fluctuation. Finally, we found that the error percentage can drop below 10% when the island size is 8.5 nm and the standard deviation of the island size is 1 nm in the absence of main pole jitter. [http://dx.doi.org/10.1063/1.4977762]

I. INTRODUCTION

It has been known that a perpendicular magnetic recording technology used in current hard disk drives is approaching its super-paramagnetic limit at about 1 Tb/in^2 (Tera-bit per square inch).[1] However, an areal density (AD) over 10 Tb/in^2 has recently become a challenge for new magnetic recording technologies.[1] A heated-dot magnetic recording (HDMR)[1,2] is a promising technology to attain this goal, which utilizes a laser to heat a bit-patterned medium (BPM) before recording data. In HDMR, a high magneto-crystalline anisotropy, K_u, material such as $L1_0$-FePt is normally utilized for a medium with small grains to keep high thermal stability.[3] Practically, a high K_u medium is needed to keep data for a long time, and a large write field strength is required to write data onto a high K_u medium. Nevertheless, a current write field value cannot exceed the limit of about 24-25 kOe.[4] Thus, the heat[4–7] or the microwave field[8–12] must be used to reduce the coercivity of magnetic media temporarily.

Near perfect bit-patterned fabrication is crucial to achieve high storage capacity in HDMR. One of the main challenges is the island size fluctuation, which could cause a written-in error during the writing process. Several methods have been presented for bit-patterned fabrication to handle the island size fluctuation. For example, a directed self-assembly of nanoparticles has been interested because of large area patterning.[13–17] Nonetheless, this technique still has some challenges such as controlling island size distribution, obtaining small island size, and fabricating perfect templates or masks.[18] Besides the island size fluctuation, the written-in error can also be caused by bit island position jitter, main pole position fluctuation, heat spot position, and so forth. Consequently, the durability of recorded-bit patterns against these effects should be taken into consideration before recording data onto a medium.

This paper investigates the effects of island arrangement (i.e., a regularly-patterned array (or square array) and a hexagonal-patterned array (or staggered array)), and island size and main pole fluctuations in the HDMR system, where the micromagnetic simulation is employed based on the

Landau-Lifshitz-Gilbert (LLG) equation and the thermal effect on BPM is evaluated by the Brillouin function.

II. MICROMAGNETIC MODELING

Fig. 1 shows the island layout of a 3×3 staggered array, where the 5th island is being written by a corner of the main pole. The $L1_0$-FePt material is used for a magnetic medium with the K_u of 4.6 MJ/m^3, the saturation magnetization, M_s, of 1125 kA/m,[19] and the internal exchange coupling of 12 pJ/m.[20] We consider a cylindrical island shape with the thickness of 10 nm, and the island pitch in both along- and across-track directions of 15 nm corresponding to an AD of 2.86 Tb/in^2.

The LLG equation is utilized to solve magnetization movement as given by[21]

$$\frac{\partial \vec{M}(\vec{r}_i,t)}{\partial t} = -|\gamma|\,\vec{M}(\vec{r}_i,t)\times\vec{H}_{eff}(\vec{r}_i,t) - \frac{|\gamma|\alpha}{M_s}\vec{M}(\vec{r}_i,t)\times\left[\vec{M}(\vec{r}_i,t)\times\vec{H}_{eff}(\vec{r}_i,t)\right], \tag{1}$$

where $\vec{M}(\vec{r}_i,t)$ is a magnetization vector, $\vec{H}_{eff}(\vec{r}_i,t)$ is an effective field consisting of anisotropy, demagnetizing, exchange and Zeeman fields, α is the Gilbert damping constant, and γ is a gyromagnetic ratio. The heating technique is handled via the Brillouin function,[22–24] which explains the relationship among K_u, M_s, and the heating temperature, T (K). Additionally, this paper assumes that the thermal profile is a Gaussian shape[25] according to

$$T = T_0 \exp\left(-\frac{r^2}{r_0^2}\ln 2\right), \tag{2}$$

where T_0 is the highest temperature set as 660 K,[26] r is the distance, and r_0 = 35 nm is a full width of the thermal profile at half its maximum.[25] Then, the change of K_u and M_s under temperature can be found by.[23,24]

$$M_s(T) = M_s(0)\left[\frac{2J+1}{2J}\coth\left(\frac{2J+1}{2J}\beta\right) - \frac{1}{2J}\coth\left(\frac{\beta}{2J}\right)\right], \tag{3}$$

$$\beta = 3\left(1-\frac{T}{T_C}\right), \tag{4}$$

$$\frac{K_u(T)}{K_u(0)} = \left[\frac{M_s(T)}{M_s(0)}\right]^n, \tag{5}$$

where J = 0.85 is a total angular momentum, T_c = 770 K is the Curie temperature of $L1_0$-FePt material, $n \approx 2$ is a factor of the thin film of $L1_0$-FePt series,[19] and $M_s(0)$ = 1125 kA/m and $K_u(0)$ = 4.6 MJ/m^3 are the M_s and the K_u at room temperature (293 K), respectively. Note that the way to treat the thermal spot was thoroughly explained in our previous work.[22]

Consider the island layout in Fig. 1, where all 9 bits are initially assumed to be the bit "–1" or pointed down in the –z direction. Thus, we assume that the 5th island (or the target island) is being written, the 1st–4th islands are the previously recorded bits (i.e., there are 16 possible data patterns as listed in Table I), and the 6th–9th islands are the next written bits. The triangular write pole[27,28] with an along-track width of 93.5 nm and an across-track length of 50.5 nm is utilized to write the

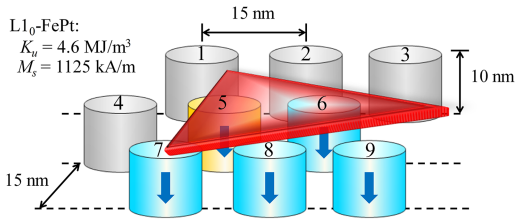

FIG. 1. Configuration of a staggered array island medium under the writer (not scaled).

TABLE I. The 16 data patterns based on the four previously recorded bits.

Track	Patterns			
	Pattern 1	Pattern 2	Pattern 3	Pattern 4
Written-track	1 1 1	1 1 -1	-1 1 1	1 -1 1
Current-track	1 **-1** -1	1 **-1** -1	1 **-1** -1	1 **-1** -1
Next-track	-1 -1 -1	-1 -1 -1	-1 -1 -1	-1 -1 -1
	Pattern 5	Pattern 6	Pattern 7	Pattern 8
Written-track	1 1 1	-1 1 -1	1 -1 -1	1 1 -1
Current-track	-1 **-1** -1	1 **-1** -1	1 **-1** -1	-1 **-1** -1
Next-track	-1 -1 -1	-1 -1 -1	-1 -1 -1	-1 -1 -1
	Pattern 9	Pattern 10	Pattern 11	Pattern 12
Written-track	1 -1 1	-1 1 1	-1 -1 1	-1 -1 -1
Current-track	-1 **-1** -1	-1 **-1** -1	1 **-1** -1	1 **-1** -1
Next-track	-1 -1 -1	-1 -1 -1	-1 -1 -1	-1 -1 -1
	Pattern 13	Pattern 14	Pattern 15	Pattern 16
Written-track	-1 1 -1	1 -1 -1	-1 -1 1	-1 -1 -1
Current-track	-1 **-1** -1	-1 **-1** -1	-1 **-1** -1	-1 **-1** -1
Next-track	-1 -1 -1	-1 -1 -1	-1 -1 -1	-1 -1 -1

data on a medium, where the gradient fields in along- and across-track directions are 500 and 483 Oe/nm, respectively. Furthermore, we suppose that the magnetic field with the amplitude of 20 kOe[22] is applied in the +z direction to magnetize the bit "+1" onto the 5th island.

III. RESULTS AND DISCUSSION

This paper investigates an error resulted from a magnetization reversal in the 1st – 5th islands during the writing process. Specifically, the error occurs when the 5th island cannot be written and/or at least one of the 1st – 4th islands is overwritten. In simulation, we rewrite the bit "+1" on the 5th island a thousand (1,000) times, where the 1st – 4th islands have been systematically analyzed each time. Hence, the number of errors is counted and averaged to obtain the error percentage. Let D be an island size (in diameter), $\bar{D}$ be a mean value of D, σ_B be a standard deviation of D, $\sigma_B/\bar{D}$ be the size fluctuation,[29] and σ_M be a standard deviation of main pole position. Moreover, we consider only the case where D varies between 4 nm to support the thermal stability of 60 and 14 nm to avoid an overlap event among bit islands.

A. Array vs. stagger

Practically, the nanodot patterning from lithography and self-assembly techniques can provide square and staggered arrays.[29] This section studies the effect of fabricated patterns on the writing performance of HDMR as illustrated in Fig. 2(a), where we choose D = 10.5 nm, σ_B = 1 nm, and σ_M = 0 (i.e., the main pole is aligned with the center of the 5th island). Clearly, a staggered array yields a lower error percentage than a square array for all data patterns, where an error occurs when the 5th island cannot be written.

In addition, we found that the four previously recorded bits (the 1st – 4th islands) have greater impact on the error performance in a staggered array than that in a square array. Because the writer geometry is triangular (see Fig. 1), the 3rd island has less impact on the 5th island than the others in the staggered array. Hence, if the effect of magnetization from the 3rd island is neglected, the 9th – 16th data patterns will have at most one recorded island, whose magnetization direction is against the 5th island. Accordingly, they will yield a writing error lower than the 1st – 8th data patterns, which have at least two recorded islands, whose magnetization directions are against the 5th island.

Results show that the magnetization states (or magnetic field) of the surrounding islands must be taken into account when designing the two-dimensional (2D) modulation code[30] to avoid the bad data patterns to be recorded onto a medium. It can also be concluded that the staggered island arrangement helps improve the error performance of the HDMR system,[31] if compared to the square

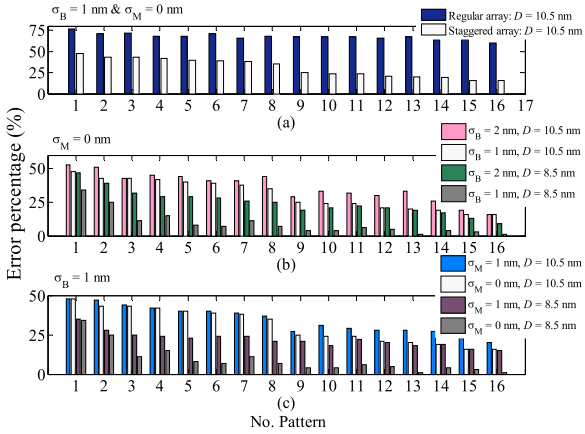

FIG. 2. Error percentage of (a) square array versus staggered array for D = 10.5 nm, σ_B = 1 nm, and $\sigma_M = 0$; (b) island size fluctuation with $\sigma_M = 0$; and (c) both island size and main pole position fluctuations with σ_B = 1 nm.

island arrangement. Therefore, from now on, we focus only on the staggered island arrangement in our next study.

B. Island size fluctuation

To study the effect of island size fluctuation, we set $\sigma_M = 0$ and investigate the case where $D \in \{8.5, 10.5\}$ and $\sigma_B \in \{1, 2\}$. Fig. 2(b) displays the error percentage of different system conditions, where the staggered array with $\sigma_B = 2$ nm still yields a lower error percentage than the square array with $\sigma_B = 1$ nm. Apparently, a larger σ_B provides a higher error percentage. Also, the smaller D and σ_B will yield better system performance. This implies that the writing error performance also relies on an island volume.[26] However, the distance and stray field should be also concerned when the writing error was investigated. Note that when D = 10.5 nm, the results are not much different because the island size variation is limited within 4 – 14 nm.

Although the heat spot size is 35 nm covering nine islands' area, we found that the error does not come from the overwritten neighboring islands. This is because the thermal profile is a Gaussian shape, where the temperature gradually decreases from its maximum value at the center of the hot spot. Consequently, the distributed heat on BPM is insufficient to reduce the coercivity of magnetic islands beneath the maximum magnetic field of the write pole.

C. Island size and main pole position fluctuations

In this case, both the island size and the main pole position are fluctuated according to Gaussian distribution. We assume that the main pole position is moved over the 5th island's area. Then, we investigate the effects of $D \in \{8.5, 10.5\}$ and $\sigma_M \in \{0, 1\}$ as shown in Fig. 2(c), where σ_B = 1 nm is considered. Here, we assume that the center of the heat spot is moved together with the main pole. For D = 10.5 nm, the system with $\sigma_M = 0$ provides an error percentage slightly lower than that with σ_M = 1 nm. However, for D = 8.5 nm, the system with $\sigma_M = 0$ can offer the error below 10%, but the error can increase up to 35% when σ_M = 1 nm. Regardless of $\sigma_M \in \{0, 1\}$, the system with D = 8.5 nm always performs better that with D = 10.5 nm. Additionally, in the presence of σ_M, the error percentages resulted from various data patterns are not much different. Thus, apart from improving and developing BPM fabrication, controlling the writer position is also an important issue to improve the HDMR system performance.

Finally, we sum all writing errors resulted from the sixteen data patterns and average them to obtain a mean value of error percentages, as depicted in Fig. 3. For the staggered island arrangement, the system with D = 8.5 nm, σ_B = 1 nm, and $\sigma_M = 0$ offers the lowest averaged error percentage (less than 10%), whereas that with D = 10.5 nm, σ_B = 2 nm, and $\sigma_M = 0$ yields the worst performance. In addition, it is apparent that the staggered island arrangement is superior to the square island arrangement.

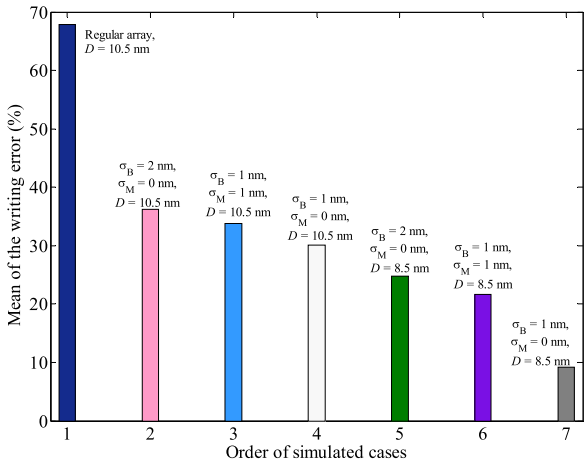

FIG. 3. Comparison of the mean of writing error percentage, which is obtained by summing all writing errors resulted from the sixteen data patterns and average them.

IV. CONCLUSION

The error event during the writing process in HDMR systems is investigated via the micromagnetic modeling based on the LLG equation. Clearly, the staggered island arrangement copes with variations to suppress writing errors better than the square island arrangement. Writing errors also depend on the previous magnetization states of neighboring islands. A drastic deviation of island size will lead to a poor writing performance, which can be alleviated by a good lithography process. A desired island size relying on a required AD has a lot of influence on reducing the writing errors. Generally, a smaller island volume yields a better error performance. In addition, we also found some destructive data patterns (according to the 1^{st} – 4^{th} islands) that easily cause an error during data recovery process. This result can be used to design the 2D modulation code to prevent the destructive data patterns to be recorded onto a medium, thus improving the overall system performance.

ACKNOWLEDGMENTS

This work was supported partly by Thailand Research Fund (TRF) under grant number PHD59I0045, College of Advanced Manufacturing Innovation, KMITL, and partly by the Research and Development Institute, Nakhon Pathom Rajabhat University, Thailand.

[1] C. Vogler, C. Abert, F. Bruckner, D. Suess, and D. Praetorius, Appl. Phys. Lett. **108**, 102406 (2016).
[2] C. Vogler, C. Abert, F. Bruckner, D. Suess, and D. Praetorius, J. Appl. Phys. **119**, 223903 (2016).
[3] S. Iwasaki, Proc. Jpn. Acad. Ser. B Phys. Biol. Sci. **85**, 37–54 (2009).
[4] M. H. Kryder, E. C. Gage, T. W. McDaniel, W. A. Challener, R. E. Rottmayer, G. Ju, Y.-T. Hsia, and M. F. Erden, Proc. IEEE **96**, 1810–1835 (2008).
[5] L. Pan and D. B. Bogy, Nat. Photon. **3**, 189–190 (2009).
[6] W. A. Challener, C. Peng, A. V. Itagi, D. Karns, W. Peng, Y. Peng, X. Yang, X. Zhu, N. J. Gokemeijer, Y.-T. Hsia, G. Ju, R. E. Rottmayer, M. A. Seigler, and E. C. Gage, Nat. Photon. **3**, 220–224 (2009).
[7] Z. Liu, Y. Jiao, and R. H. Victora, Appl. Phys. Lett. **108**, 232402 (2016).
[8] J.-G. Zhu, X. Zhu, and Y. Tang, IEEE Trans. Magn. **44**, 125–131 (2008).
[9] J.-G. Zhu and Y. wang, IEEE Trans. Magn. **46**, 751–757 (2010).
[10] K. Rivkin, M. Benakli, N. Tabat, and H. Yin, J. Appl. Phys. **115**, 214312 (2014).
[11] S. Okamoto, N. Kikuchi, M. Furuta, O. Kitakami, and T. Shimatsu, J. Phys. D: Appl. Phys. **48**, 353001 (2015).
[12] T. Tanaka, S. Kashiwagi, Y. Kanai, and K. Matsuyama, J. Magn. Magn. Matter. **416**, 188–193 (2016).
[13] R. Sbiaa and S. N. Piramanayagam, Recent Pat. Nanotech. **1**, 29–40 (2007).
[14] R. A. Griffiths, A. Williams, C. Oakland, J. Roberts, A. Vijayaraghavan, and T. Thomson, J. Phys. D: Appl. Phys. **46**, 503001 (2013).
[15] Z. Li, W. Zhang, and K. M. Krishnan, AIP Adv. **5**, 087165 (2015).
[16] E. Yang, Z. Liu, H. Arora, T.-W. Wu, V. Ayanoor-Vitikkate, D. Spoddig, D. Bedau, M. Grobis, B. A. Gurney, T. R. Albrecht, and B. Terris, Nano Lett. **16**, 4726–4730 (2016).
[17] A. M. Abdelgawad, S. D. Oberdick, and S. A. Majetich, AIP Adv. **6**, 056114 (2016).
[18] A. Kikitsu, T. Maeda, H. Hieda, R. Yamamoto, N. Kihara, and Y. Kamata, IEEE Trans. Magn. **49**, 693–698 (2013).

[19] J. U. Thiele, K. R. Coffey, M. F. Toney, J. A. Hedstrom, and A. J. Kellock, J. Appl. Phys. **91**, 6595 (2002).
[20] W. Tipcharoen, A. Kaewrawang, and A. Siritaratiwat, Adv. Mater. Sci. Eng. **2015**, 504628.
[21] J. Zhang, Y. Liu, F. Wang, J. Zhang, R. Zhang, Z. Wang, and X. Xu, J. Appl. Phys. **111**, 073910 (2012).
[22] W. Tipcharoen, C. Warisarn, A. Kaewrawang, and P. Kovintavewat, Jpn. J. Appl. Phys. **55**, 07MB01 (2016).
[23] F. Akagi, M. Mukoh, M. Mochizuki, J. Ushiyama, T. Matsumoto, and H. Miyamoto, J. Magn. Magn. Mater. **324**, 309–313 (2012).
[24] F. Akagi, T. Matsumoto, and K. Nakamura, J. Appl. Phys. **101**, 09H501 (2007).
[25] B. X. Xu, Z. J. Liu, R. Ji, Y. T. Toh, J. F. Hu, J. M. Li, J. Zhang, K. D. Ye, and C. W. Chia, J. Appl. Phys. **111**, 07B701 (2012).
[26] W. Tipcharoen, C. Warisarn, and P. Kovintavewat, IEEE Magn. Lett. **7**, 4505404 (2016).
[27] M. Yamashita, Y. Okamoto, Y. Nakamura, H. Osawa, K. Miura, S. Greaves, H. Aoi, Y. Kanai, and H. Muraoka, J. Appl. Phys. **111**, 07B727 (2012).
[28] M. Yamashita, Y. Okamoto, Y. Nakamura, H. Osawa, K. Miura, S. J. Greaves, H. Aoi, Y. Kanai, and H. Muraoka, IEEE Trans. Magn. **48**, 4586–4589 (2012).
[29] M. Asbahi, K. T. P. Lim, F. Wang, M. Y. Lin, K. S. Chan, B. Wu, V. Ng, and J. K. W. Yang, IEEE Trans. Magn. **50**, 3200405 (2014).
[30] A. Arrayangkool and C. Warisarn, J. Appl. Phys. **117**, 17A904 (2015).
[31] P. W. Nutter, I. T. Ntokas, B. K. Middleton, and D. T. Wilton, IEEE Trans. Magn. **41**, 3214–3216 (2005).